Progress Report for SCEC project, "Sequences of Cascading Elastodynamic Ruptures on Geometrically Complex Faults: Rupture Initiation, Propagation, Termination, and Variation" 2005, $25,000, PI: B.E. Shaw

The main thrust of this work is to seek a deeper understanding of the dynamics of earthquakes on fault systems. Results from support of this grant are still being developed. In the last year, three papers have been published, and two papers have been submitted for publication. Below, some results of the published papers are briefly mentioned, and figures from the most directly relevant submitted paper is highlighted.

"Dynamic Heterogeneities Versus Fixed Heterogeneities in Earthquake Models", [Shaw, 2004a], *Geophysical Journal International, 156***, 275, doi:10.1111/j.1365-246X.2003.02134.x** . We examine the interaction of dynamics with fixed material heterogeneities on a planar fault. The paper addresses the following issues. A debate has raged over whether fixed material and geometrical heterogeneities or alternatively dynamic stress heterogeneities arising through frictional instabilities dominate earthquake complexity. It may also be that both types of heterogeneities interact and are important. Here, we examine frictions which produce complex attractors on homogeneous faults, and study them on heterogeneous faults, in order to study the interaction of dynamic stress heterogeneities and fixed fault heterogeneities. We consider two types of fixed heterogeneities: an additive noise and a multiplicative noise to the frictional strength of the fault. Because of the linearity of the bulk elastodynamics, the attractor is unaffected by additive fixed noise in the strength of the fault: adding an arbitrary function of space, fixed in time, to the friction leaves the resulting attractor unchanged. In contrast, multiplicative fixed noise multiplying the friction can have a profound effect on the resulting attractor. In the small multiplicative noise amplitude limit, the frictional weakening attractor is little perturbed; at finite amplitudes, fixed heterogeneities substantially alter the attractor. We see, as one consequence, a shift toward longer length events at larger amplitudes. Fixed heterogeneities are seen to reduce the irregularities created by the frictional instability we study, but by no means destroy them. We quantify this by examining a measure of variability of importance to hazard, the coefficient of variation of large event recurrence times. The coefficient of variation is seen to remain substantial even for large fixed heterogeneities. For all frictions examined, at low fixed heterogeneity the stress concentrations left over by the ends of the large events dominate where most of the small events occur, while at higher heterogeneity the stress irregularities left over by fixed fault heterogeneities begin to dominate where the small events occur. This may be the strongest signature of fixed heterogeneities, and should be examined further in the Earth.

"Self-organizing fault systems and self-organizing elastodynamic events on them: Geometry and the distribution of sizes of events", [Shaw, 2004b], *Geophysical Research Letters, 31***, L17603, doi:10.1029/2004GL019726.** . We introduce a new model which both generates a self-organizing complex segmented fault system which then accommodates finite

strain, and generates sequences of elastodynamic events on that complex fault system. This opens up a new realm of study of populations of cascading elastodynamic ruptures on complex fault systems. We examine the distribution of sizes of events in the model, and its dependence on fault geometry. We see an evolution from a more Gutenberg-Richter like distribution of events at smaller strains to a more characteristic like distribution at larger strains. The distribution of lengths of events is not a simple scaling of the distribution of lengths of segments. We see relative insensitivity of the distribution of sizes of events to the friction used. Examining the distributions of sizes of events on fault segments of different lengths, we find support for a modified segmentation hypothesis whereby segments both break in power law small events and occasionally participate in cascading multisegment larger ruptures, but also predominantly break as a unit.

"Variation of large elastodynamic earthquakes on complex fault systems", [Shaw, 2004c], *Geophysical Research Letters, 31* **L18609, doi:10.1029/2004GL019943** . One of the biggest assumptions, and a source of some of the biggest uncertainties in earthquake hazard estimation is the role of fault segmentation in controlling large earthquake ruptures. Here we apply a new model which produces sequences of elastodynamic earthquake events on complex segmented fault systems, and use these simulations to quantify the variation of large events. We find a number of important systematic effects of segment geometry on the slip variation and the repeat time variation of large events, including an increase in variation at the ends of segments and a decrease in variation for the longest segments. Interestingly, there are both quantitative and qualitative differences between slip variation and time variation, so slip variation and time variation are not simple proxies for eachother.

"Estimating stress heterogeneity from aftershock rate", [Helmstetter and Shaw, 2005], submitted. We estimate the rate of aftershocks triggered by a heterogeneous stress change, using the rate-and-state model of *Dieterich* [1994]. We show than an exponential stress distribution $P(\tau) \sim \exp(-\tau/\tau_0)$ gives an Omori law decay of aftershocks with time $\sim 1/t^p$, with an exponent $p = 1 - A\sigma_n/\tau_0$, where A is a parameter of the rate-and-state friction law, and σ_n the normal stress. Omori exponent p thus decreases if the stress "heterogeneity" τ_0 decreases. We also invert the stress distribution $P(\tau)$ from the seismicity rate $R(t)$, assuming that the stress does not change with time. We apply this method to a synthetic stress map, using the (modified) scale invariant "k^2" slip model [Herrero and Bernard, 1994]. We generate synthetic aftershock catalogs from this stress change. The seismicity rate on the rupture area shows a huge increase at short times, even if the stress decreases on average. Aftershocks are clustered in the regions of low slip, but the spatial distribution is more diffuse than for a simple slip dislocation. Because the stress field is very heterogeneous, there are many patches of positive stress changes everywhere on the fault. This stochastic slip model gives a Gaussian stress distribution, but nevertheless produces an aftershock rate which is very close to Omori's law, with an effective $p \leq 1$, which increases slowly with time. The inversion of the full stress distribution $P(\tau)$ is badly constrained for negative stress values, and for very large positive values, if the time interval of the catalog is limited. However, constraining $P(\tau)$ to be a Gaussian distribution allows

a good estimation of $P(\tau)$ for a limited number of events and catalog duration. We show that stress shadows are very difficult to observe in a heterogeneous stress context.

"Initiation propagation and termination of elastodynamic ruptures associated with segmentation of faults and shaking hazard", [Shaw, 2005], submitted . Using a model of a complex fault system, we examine the initiation, propagation, and termination of ruptures, and their relationship to fault geometry and shaking hazard. We find concentrations of epicenters near fault stepovers and ends; concentrations of terminations near fault ends; and persistent propagation directivity effects. Taking advantage of long sequences of dynamic events, we directly measure shaking hazards, such as peak ground acceleration exceedance probabilities, without need for additional assumptions. This provides a new tool for exploring shaking hazard from a physics-based perspective, its dependence on various physical parameters, and its correlation with other geological and seismological observables. Using this capability, we find some significant aspects of the shaking hazard can be anticipated by measures of the epicenters. In particular, asymmetries in the relative peak ground motion hazard along the faults appear well correlated with asymmetries in epicentral locations.

Figure 1 shows four different views of the complex sequences which develop, and the long catalogue of dynamic ruptures which occur on it. Figure 1a shows the slip rates on the faults. Figure 1b shows the density of epicenters. Figure 1c shows the density of rupture terminations. Note the association of the rupture initiations and terminations with segment ends. Figure 1d shows the rupture directivity fraction, the fraction of events propagating up or down. Note the dearth of neutral green colors in the figure where the propagation fraction is near zero, meaning only rarely do locations not have a preferred propagation direction.

Utilizing a long catalogue of dynamic events, we can make a hazard map for the fault system, combining thousands of dynamic ruptures measured individually. Figure 2a plots a standard measure of hazard, the peak acceleration for a given probability of occurrence. We measure this in the model by keeping track of peak acceleration at every point in space from each event, combining all the events to make at every point a histogram of these values. Then, choosing a probability value, we plot the acceleration level at which that probability value is exceeded over the long catalogue.

Figure 2b shows the peak velocity for the same probability of occurrence as in Figure 2a (the analogue of the 2% probability of exceedance in 50 year national hazard maps [see also http://eqhazmaps.usgs.gov]). Note the strong similarity with Figure 2a, albeit slightly less concentrated near the faults.

The last measure of shaking we show in Figure 2c is the average of kinetic energy. Note, in contrast with the peak motion curves in Figures 2a and 2b, the kinetic energy is much more symmetric along the fault, and much more concentrated along the largest faults. Thus Figure 2c is best anticipated by Figure 1a, the total slip rate on faults. The shaking maps, on the other hand, reflect rupture initiation, propagation, and termination effects in Figures 1b, 1c, and Figure 1d .

A different way of plotting the results are shown in Figure 3 where we plot the probability of a given shaking being exceeded. This alternative way of looking at the hazard shows much more interaction between faults, with nearby faults enhancing the hazard since the frequency of large

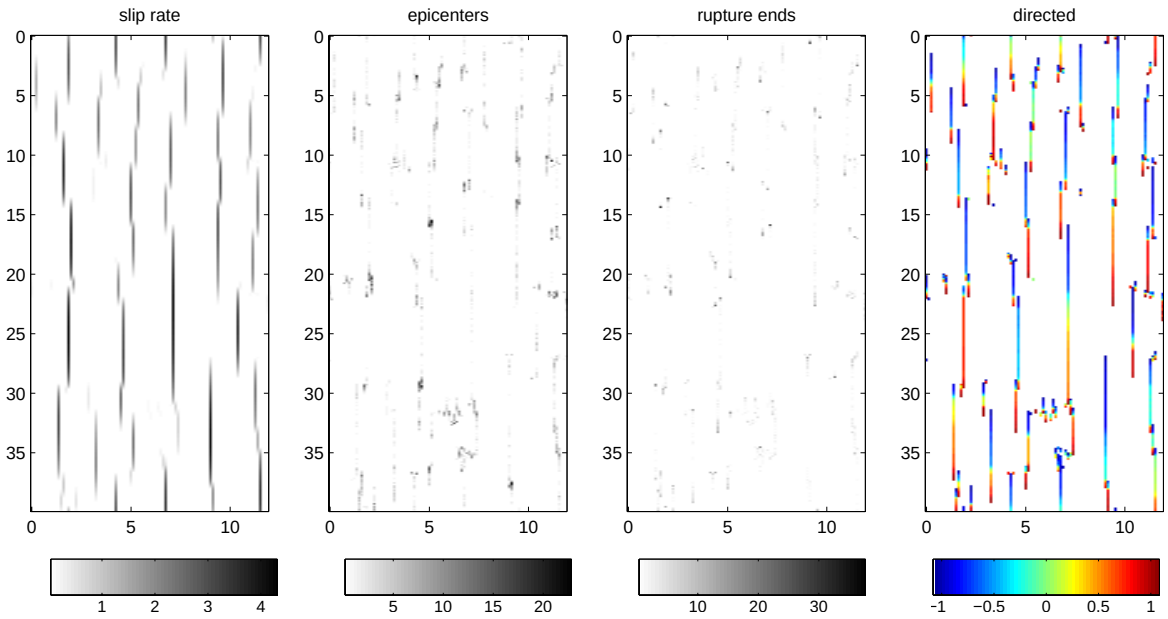

Figure 1: Four views of a long catalogue of events. (a) Slip rate per unit strain. (b) Epicentral density. (c) Rupture termination density. (d) Directivity of ruptures; fraction of events propagating up (blue colors) versus down (red colors). Note the association of epicenters with segment stepovers and ends, and the association of rupture terminations with segment ends. Note, in (d), high amplitudes– persistent directivity– is the typical, rather than exceptional case. Numbers on the horizontal and vertical axes are distances in units of the brittle crust depth, corresponding to unscaled lengths of order a few hundred km across by a thousand km long. Scale bars below the figures indicate greyscale levels.

shaking is increased. Segment stepovers show up as particularly “hot spots” from this measure. There is also the odd but nevertheless real effect of the largest faults showing a somewhat lowered relative hazard due to the very large but less frequenct great events, an effect seen in real faults as well. Figure 3 is a less standard way of representing hazard, and in addition shows much more variability spatially with changing threshold. The comparisons with both ways of representing the hazard are, however, quite interesting; and our ability to simulate both directly from physical models is a new tool for exploring their relationships. These models are, to the best of our knowledge, the first models capable of generating hazard maps directly from a physics based model, with no statistical parameterizations (such as attenuation relationships) needed. While they clearly do not yet contain all of the relevant physics, and more physical effects could and should be added, they do provide a powerful new tool for exploring shaking hazard.

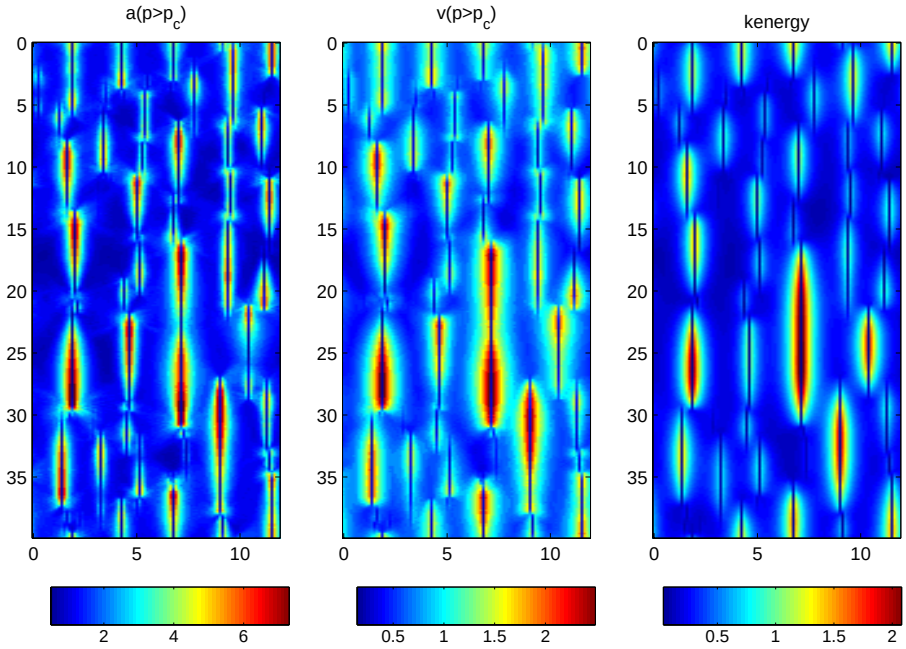

Figure 2: Shaking measures measured directly from long sequence of dynamic events. (a) Peak acceleration for $p > p_c$, with $p_c = .2$. (b) Peak velocity for $p > p_c$, with $p_c = .2$. (c) Kinetic energy. Note similar maps of peak accelerations and peak velocity, showing significant directivity effects, as contrasted with the more symmetric kinetic energy map.

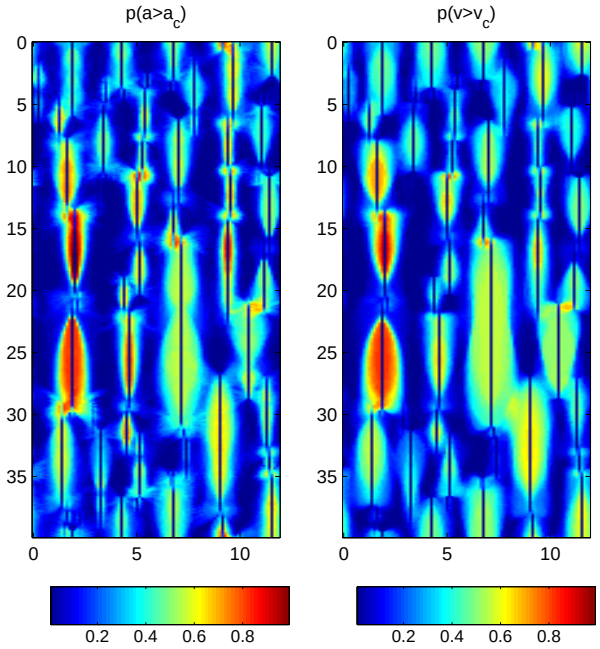

Figure 3: Shaking measures measured directly from long sequence of dynamic events. (a) Probability of peak acceleration exceeding critical acceleration, with critical acceleration chosen to have total average probability of exceedance of $p = .2$. (b) Probability of peak velocity exceeding critical velocity, with critical velocity chosen to have total average probability of exceedance of $p = .2$.